Journal of Applied Mechanics and Technical Physics, Vol. 48, No. 1, pp. 1–6, 2007

GAS FLOW ACTIVATED IN AN ELECTRON-BEAM PLASMA

V. O. Konstantinov and S. Ya. Khmel

UDC 533.9:621.039.66, 539.23+546.28

Probe measurements of electron temperature and density, electron energy distribution functions, and plasma potential in a free gas jet activated in an electron-beam plasma and in a planar reactor are presented. The measurements are performed by single, double, and triple electrostatic probes in jets of helium–argon and helium–argon–monosilane gas mixtures. The latter mixture is used to deposit films of microcrystalline and epitaxial silicon. Microcrystalline silicon films of higher quality are obtained in a dense ($n_e \approx 10^{17}$ m^{-3}) and cold ($T_e \approx 1.0$–0.5 eV) plasma with a low potential ($U_{sp} \approx 10$ V), whereas the growth of monocrystalline silicon films requires a hotter plasma ($T_e \approx 3$–5 eV) with a potential $U_{sp} \approx 15$ V.

Key words: *probe diagnostics, electron-beam plasma, chemical vapor deposition of thin silicon films.*

Introduction. Deposition of thin films often involves chemical vapor methods with activation of gaseous reagents in a discharge plasma or electron-beam plasma [1, 2]. In particular, a silane plasma is used for silicon-film deposition [3–5]. The study of such a plasma is an urgent problem, and one of the most widely used diagnostic methods is the Langmuir probe [6–8]. Probe characteristics can yield information on the electron temperature, electron density, plasma potential, and, in the general case, the electron energy distribution function. If a single or a double probe is used, however, it is impossible to determine instantaneous values of plasma parameters (measuring and processing of the current–voltage characteristic is a rather long procedure). Such information can be obtained by a triple probe [8].

It was demonstrated [9] by means of probe diagnostics that the temperature and density of secondary electrons in a nitrogen electron-beam plasma are 0.5–2.5 eV and 10^{16}–10^{17} m^{-3}, respectively. The temperature was found to decrease and the density was found to increase with increasing pressure in the electron-beam plasma. The measurements performed in an argon electron-beam plasma [10] showed that the electron temperature is approximately 1 eV, the electron density is $5 \cdot 10^{16}$ to $5 \cdot 10^{17}$ m^{-3}, and the plasma potential is approximately 4 V. Such a plasma produces a soft and nondestructive effect on the surface and can be used for material processing and depositing high-quality thin films [2]. Deposition of epitaxial layers requires a harder plasma, but a principally important quantity in this case is the plasma potential [11].

In a reactive plasma, the probe surface is contaminated by growing films; hence, correct measurements in such a plasma are ensured by using heated probes [7]. It was found in [12] with the use of heated probes that the electron temperature and density decrease with increasing flow rate of monosilane or pressure in the discharge chamber.

The present paper describes investigations performed in free jets of helium–argon and helium–argon–monosilane mixtures activated in an electron-beam plasma and in a gas flow inside a planar reactor. The goal of the present work was to determine, by means of probe diagnostics, the optimal parameters of the plasma for depositing microcrystalline and epitaxial silicon films.

Experimental Setup and Technique. The experiments were performed in a low-density gas-dynamic setup at the Institute of Thermophysics of the Siberian Division of the Russian Academy of Sciences. A sketch

Kutateladze Institute of Thermophysics, Siberian Division, Russian Academy of Sciences, Novosibirsk 630090; khmel@itp.nsc.ru. Translated from Prikladnaya Mekhanika i Tekhnicheskaya Fizika, Vol. 48, No. 1, pp. 3–10, January–February, 2007. Original article submitted November 24, 2005; revision submitted March 31, 2006.

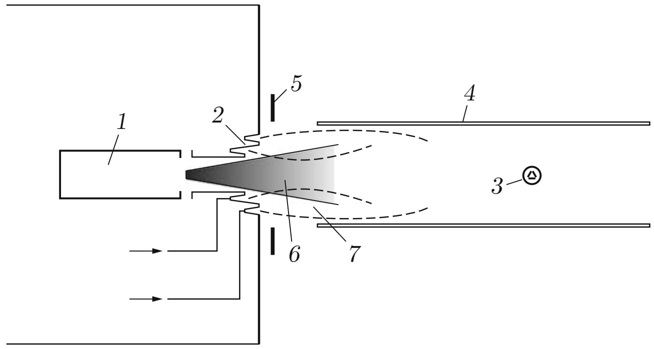

Fig. 1. Experimental setup: 1) electron gun with a plasma cathode; 2) set of ring nozzles; 3) Langmuir probe; 4) reactor; 5) additional ring electrode; 6) electron beam; 7) gas jet; the dashed curves indicate the jet boundaries.

of the experiment is shown in Fig. 1. The plasma generator was a jet source consisting of an electron gun with a plasma cathode and a double axisymmetric supersonic ring nozzle [13]. The outer diameters of the nozzles were 28 and 18 mm, the throat height was 1 mm, and the gas between the plates in the reactor was 35 mm. A mixture of processing gases (argon and monosilane) was injected through the outer ring nozzle into the vacuum chamber, and helium that served to protect the electron gun was injected through the inner ring nozzle. The flow rates of the gases were controlled by MKS Instruments flow-rate controllers. Thus, the gaseous helium–argon and helium–argon–monosilane jets were formed. The pressure in the vacuum chamber was sustained at 0.1–1.5 Pa, depending on the gas flow rate. An additional ring electrode mounted behind the nozzle served to alter the ion energy. Silicon films were deposited in a planar reactor (see Fig. 1).

To find the optimal conditions of film deposition, the parameters of the system were varied within the following ranges: beam energy $E = 0.6$–2.0 keV, beam current $I = 170$–400 mA, flow rate of argon $G_{\rm Ar} = 0$–12 liters/min, and flow rate of monosilane $G_{\rm SiH_4} = 0$–0.2 liter/min (here and below 1 liter refers to a liter of the gas at $T = 273$ K and $p = 101,325$ Pa). In the present work, we used single, double, heated double, triple, and heated triple tungsten probes 0.15–0.35 mm in diameter and 4–15 mm long. The probe was attached to a two-component traversing gear 5 mm below the beam axis to avoid possible damage owing to the action of the electron beam. The parameters measured in the experiment were the electron temperature and density in a free jet and in a planar reactor at a fixed distance from the nozzle exit in two situations: 1) unchanged beam current and varied flow rate and composition of the gas; 2) unchanged flow rate and composition of the gas and varied current. In addition, the transverse profiles of the electron temperature and density were also measured. In some tests, the Langmuir probe was used to measure or estimate the plasma potential and the electron energy distribution function [6].

Experimental Results and Discussion. Figure 2 shows the electron temperature and density as functions of the flow rate (pressure) of argon, which were obtained by a double probe in a helium–argon electron-beam plasma at a distance of 150 mm from the nozzle exit in a free jet and at a distance of 80 mm in a reactor ($E = 0.6$ keV and $I = 170$ mA). As the flow rate of argon increases, the electron temperature decreases, which may be caused by scattering and degradation of the electron beam near the nozzle exit. According to our estimates, the mean free path of electrons near the nozzle exit decreases to 1 mm with increasing flow rate of argon, and the electrons lose their energy in collisions. At $G_{\rm Ar} \approx 4$ liters/min in the free jet and at $G_{\rm Ar} \approx 2$ liters/min in the reactor, the electron beam seems to be completely scattered, and the temperature becomes constant. The electron temperature in the reactor reaches a constant value faster than that in the free jet. The reason may be a shock wave formed in the reactor, which leads to an increase in density and, as a consequence, additional scattering of electrons. Such a behavior of temperature suggests that the main ionization region is located near the nozzle exit. As the argon flow rate increases, the electron density drastically increases and reaches approximately identical values in the free jet and in the reactor at high flow rates. Figure 2 also shows the data obtained in [9]. As the measurements in [9] were performed under static conditions in an electron-beam plasma in nitrogen environment, the results can be compared by using the pressure of the background gas. A comparison with the reactor conditions is more correct,

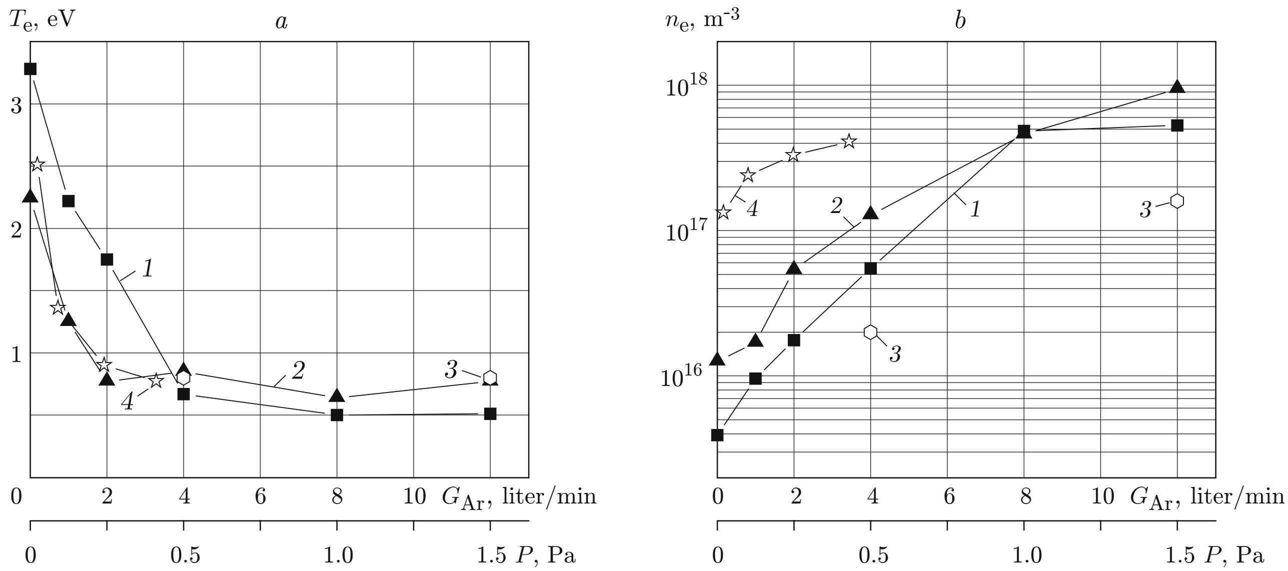

Fig. 2. Electron temperature (a) and density (b) as functions of the flow rate (pressure) of the gas: points 1–3 refer to the data obtained in the present work in a free jet (1), in a reactor (2), and in a reactor with $G_{SiH_4} = 0.2$ liter/min (3); points 4 refer to the data of [9].

because a shock wave is formed at the reactor entrance, the flow becomes subsonic, and the pressure is close to the background value. It is seen in Fig. 2a that the electron temperatures are in good agreement. This means that the gas pressure or, more exactly, the gas density is the governing parameter for the electron temperature if the distance from the measurement point is large, as compared with the mean free path of electrons. The electron density in [9] is substantially higher, because the beam current is higher approximately by an order of magnitude, and the beam energy is lower. In both cases, however, the electron density increases with increasing gas pressure.

Publications suggest that a dense plasma with an electron temperature $T_e \approx 1$ eV is favorable for deposition of thin films; therefore, the measurements in the helium–argon–monosilane mixture were performed for $G_{Ar} = 4$–12 st. liters/min with monosilane addition ($G_{SiH_4} = 0.2$ liter/min). It is seen in Fig. 2 that monosilane addition to the carrier gas significantly reduces the electron density, whereas the temperature remains almost unchanged. The grown silicon films were microcrystalline ones, but the degree of crystallinity (crystallization) is substantially higher and its gradient is lower at high flow rates [4]. Apparently, the reasons are better screening of the growing film surface from high-energy particles, on one hand, and better mixing of the activated flow behind the shock wave, on the other hand.

Figure 3 shows the electron density and temperature as functions of the beam current, which were obtained by a double probe in a helium–argon electron-beam plasma at a distance of 80 mm from the nozzle exit in the reactor ($E = 0.6$ keV and $G_{Ar} = 4$ liters/min). As the beam current increases, the electron temperature changes insignificantly, whereas the electron density increases. Thus, the electron density in an electron-beam plasma can be changed without changing the electron energy distribution function. Figure 3 also shows the data of [14] for an electron-beam nitrogen plasma. Though the beam current in [14] is higher approximately by an order of magnitude (see Fig. 3b), the electron density differs insignificantly. This can be attributed to the higher gas density (by an order of magnitude) in the present work, as compared with that in [14]. The character of the dependences is identical in both cases.

To validate the data obtained by a double probe, the measurements were also performed by a single Langmuir probe in the reactor at $E = 0.6$ keV, $I = 170$ mA, and $G_{Ar} = 4$ liters/min. The values $T_e = 1.1$ eV and $n_e = 8 \cdot 10^{16}$ m^{-3} agree with the data obtained by a double probe ($T_e = 0.9$ eV and $n_e = 1.3 \cdot 10^{17}$ m^{-3}) within the measurement error, which was 20% (for temperature). The plasma potential based on the current–voltage diagram was 10 V. Figure 4 shows the electron energy distribution function N, which was calculated by the current–voltage diagram, and the Maxwell and Druyvesteyn distribution functions for the same mean energy. The measured distribution is fairly close to the Druyvesteyn distribution function. This means that processes with

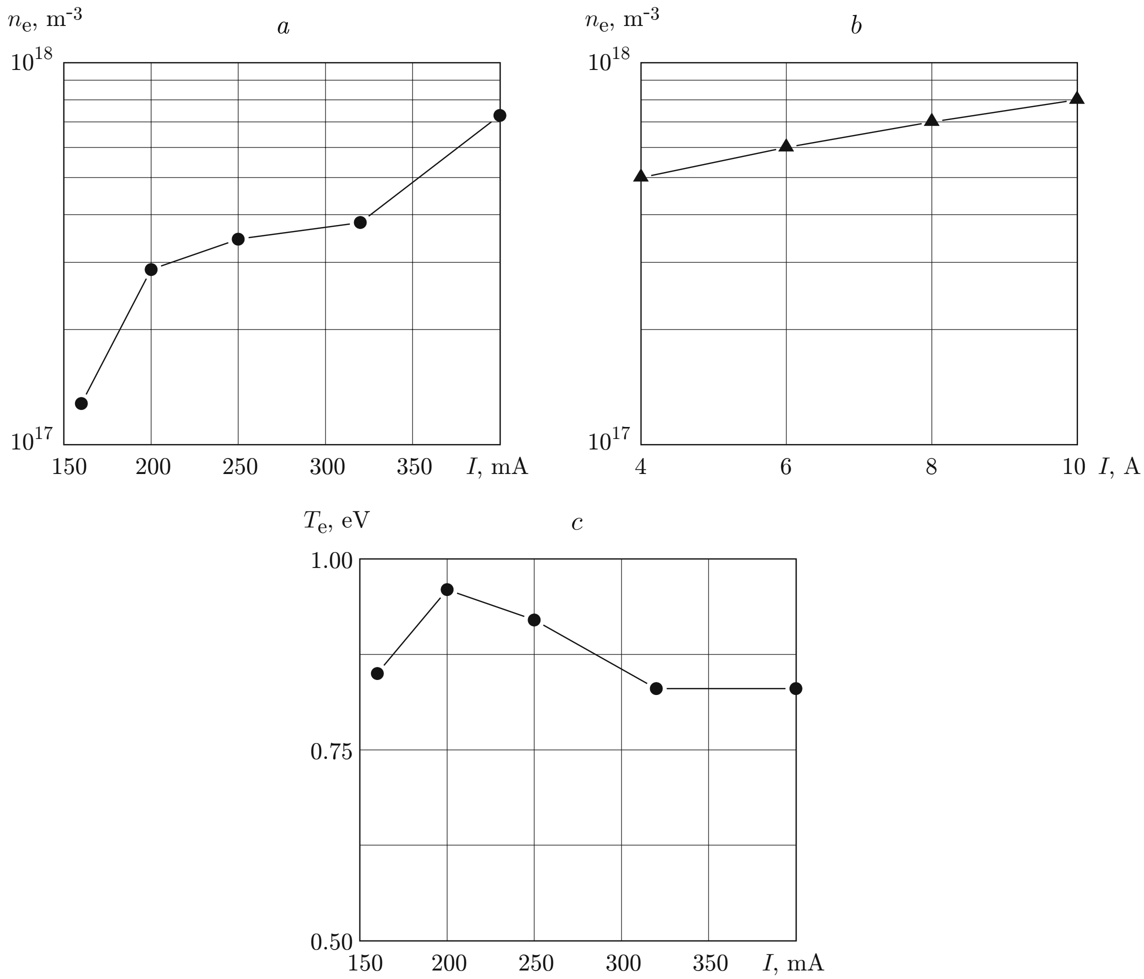

Fig. 3. Electron density (a and b) and temperature (c) versus the beam current: the data of the present work are shown by the curves in Figs. 3a and 3c; the curve in Fig. 3b shows the data of [14].

a high threshold proceed in the plasma, which "suppress" high-energy electrons in the distribution function [7]. The electron temperature based on the electron energy distribution function was 1 eV, which is consistent with the above-given values.

Thus, under certain parameters of the jet source ($G_{\mathrm{Ar}} = 4$–12 liters/min, $G_{\mathrm{SiH_4}} = 0.2$ liter/min, $E = 0.6$ keV, and $I = 170$ mA), it is possible to obtain a cold ($T_{\mathrm{e}} \approx 0.5$–$1.0$ eV) high-density ($n_{\mathrm{e}} \approx 10^{17}$ m^{-3}), and low-potential ($U_{sp} \approx 10$ V) electron-beam plasma near the substrate, which is suitable for deposition of microcrystalline silicon films.

For growing epitaxial silicon films by chemical vapor methods at reduced temperatures, one has to ensure elevated mobility of adsorbed silicon atoms on the surface of the growing film and remove hydrogen atoms from this surface [11, 15]. Hence, the plasma should supply a substantial energy flux to the film surface and, correspondingly, have harder parameters than those in the case considered above. The plasma potential, however, should not exceed 15 V [11] to avoid damaging of the growing film surface by high-energy ions. Epitaxial silicon films were grown at $E = 1.5$ keV and $I = 300$ mA. A heated triple probe had to be used because of the high growth rate of the films and, correspondingly, short duration of the experiment. Reliability of data obtained by the triple probe was preliminary verified by a double probe.

Figure 5 shows the transverse profiles of the electron temperature and density, which were obtained in helium–argon and helium–argon–monosilane electron-beam plasmas at a distance of 130 mm from the nozzle exit in the reactor. For the lower flow rate of argon, the electron temperature and density in the center are significantly

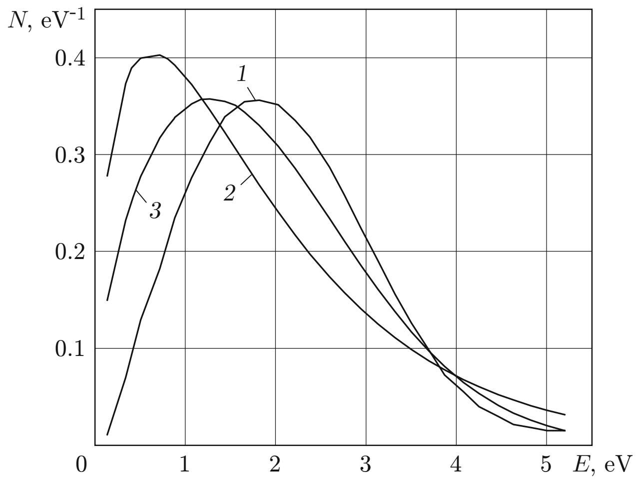

Fig. 4. Electron energy distribution function: curve 1 shows the data of the present work, curve 2 is the Maxwellian distribution, and curve 3 is the Druyvesteyn distribution.

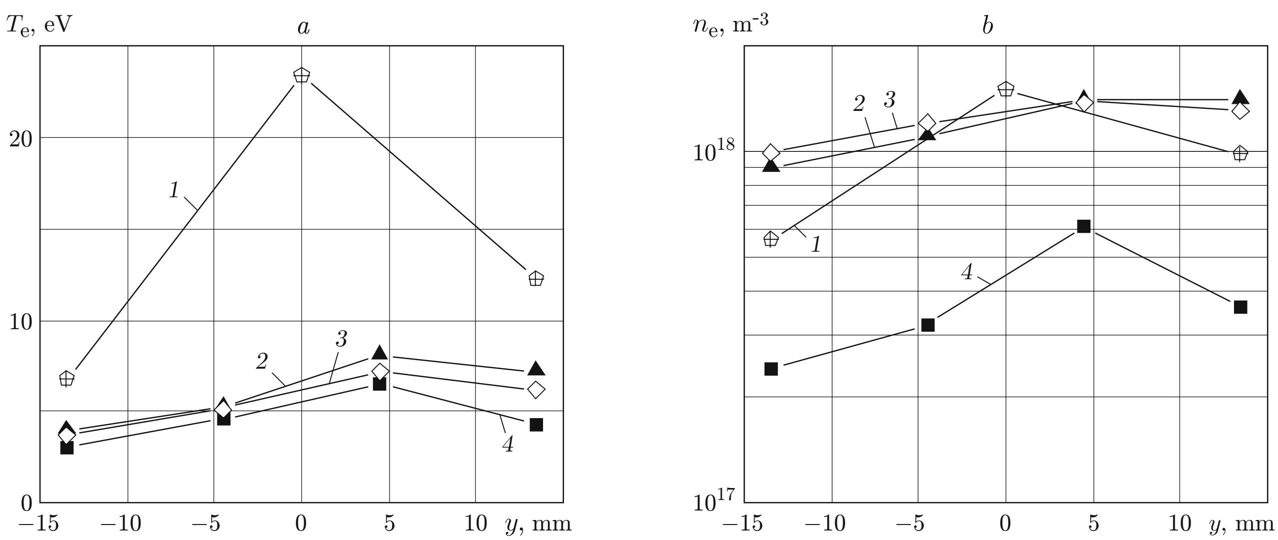

Fig. 5. Electron temperature (a) and density (b) versus the transverse coordinate: 1) $G_{\mathrm{Ar}} = 4$ liters/min, $G_{\mathrm{SiH_4}} = 0$, and $U = 0$; 2) $G_{\mathrm{Ar}} = 12$ liters/min, $G_{\mathrm{SiH_4}} = 0$, and $U = 0$; 3) $G_{\mathrm{Ar}} = 12$ liters/min, $G_{\mathrm{SiH_4}} = 0$, and $U = 30$ V; 4) $G_{\mathrm{Ar}} = 12$ liters/min, $G_{\mathrm{SiH_4}} = 0.2$ liters/min, and $U = 30$ V.

higher than those at the periphery, which is caused by the presence of the electron beam. For $G_{\mathrm{Ar}} = 12$ liters/min, however, spatial inhomogeneities are almost eliminated, which seems to be caused by significant scattering of primary electrons. As previously, the electron temperature decreases and the electron density increases with increasing flow rate of argon. If the helium–argon mixture is diluted by monosilane, the electron density decreases to a large extent, whereas the electron temperature decreases only slightly. The electron temperature and density change insignificantly if a positive potential U is applied to the ring electrode.

The plasma potential was estimated on the basis of the floating potential of a single probe and the electron temperature. For $G_{\mathrm{Ar}} = 12$ liters/min, the potential decreases to 15 V when moving from the beam axis to the substrate. Silicon films grown at $G_{\mathrm{Ar}} = 4$ liters/min and $G_{\mathrm{SiH_4}} = 0.2$ liter/min have a polycrystalline structure, and those grown at $G_{\mathrm{Ar}} = 12$ liters/min are textured polycrystalline films; epitaxial silicon could be obtained only with additional supply of a positive potential equal to 30 V onto the ring electrode. Thus, variation of the argon flow rate exerts a significant effect on the electron temperature (and plasma potential), whereas application of an electric potential onto the ring electrode allows more refined tuning of the system.

Thus, harder conditions ($G_{\mathrm{Ar}} = 12$ liters/min, $G_{\mathrm{SiH_4}} = 0.2$ liter/min, $E = 1.5$ keV, and $I = 300$ mA) ensure the formation of a hotter ($T_{\mathrm{e}} \approx 3$–5 eV) and denser ($n_{\mathrm{e}} \approx 10^{17}$ m^{-3}) plasma with a potential close to 15 V necessary for obtaining epitaxial layers of silicon.

Conclusions. The probe technique is used to measure the electron temperature and density, the electron energy distribution functions, and the plasma potential in a free gas jet activated in an electron-beam plasma and in a planar reactor.

As the argon flow rate increases, the electron temperature is found to drastically decrease and then reach a constant value, whereas the electron density increases, and the ionization region is shifted toward the nozzle exit. The electron temperature changes insignificantly and the density increases with increasing beam current, Hence the electron density in an electron-beam plasma can be altered without changing the electron energy distribution function. Dilution of a helium–argon mixture by monosilane significantly reduces the electron density and has almost no effect on the electron temperature. It follows from the experimental results that certain parameters of the system ($G_{\mathrm{Ar}} = 4$–12 liters/min, $G_{\mathrm{SiH_4}} = 0.2$ liter/min, $E = 0.6$ keV, and $I = 170$ mA) can ensure the formation of a cold ($T_{\mathrm{e}} \approx 0.5$–1.0 eV) and dense ($n_{\mathrm{e}} \approx 10^{17}$ m^{-3}) electron-beam plasma with a low potential ($U_{sp} \approx 10$ V), which can be used for depositing thin films of microcrystalline silicon. Growing of epitaxial films requires the use of a hotter plasma ($T_{\mathrm{e}} \approx 3$–5 eV) whose potential should be close to $U_{sp} = 15$ V but not exceed this value.

REFERENCES

1. K. L. Choy, "Chemical vapour deposition of coatings," *Prog. Mater. Sci.*, **48**, No. 2, 57–170 (2003).
2. A. Ito, R. Miyano, R. Kitada, et al., "Production of high-density plasmas in electron-beam-excited plasma device," *Jpn. J. Appl. Phys, Pt. 1*, **33**, No. 7B, 4239–4242 (1994).
3. J. K. Rath, "Low temperature polycrystalline silicon: a review on deposition, physical properties and solar cell applications," *Solar Energ. Mater. Solar Cells*, **76**, No. 4, 431–487 (2003).
4. R. G. Sharafutdinov, S. Ya. Khmel, V. G. Shchukin, et al., "Gas-jet electron beam plasma chemical vapor deposition method for solar cell application," *Solar Energ. Mater. Solar Cells*, **89**, Nos. 2/3, 99–111 (2005).
5. M. Imaizumi, K. Okitsu, M. Yamaguchi, et al., "Growth of microcrystalline silicon film by electron beam excited plasma chemical vapor deposition without hydrogen dilution," *J. Vac. Sci. Technol., Ser. A*, **16**, No. 5, 3134–3137 (1998).
6. R. Huddelstone and S. Leonard (eds.), *Plasma Diagnostic Techniques*, New York (1967).
7. Yu. A. Ivanov, Yu. A. Lebedev, and L. S. Polak, *Contact Diagnostic Methods in Nonequilibrium Plasma Chemistry* [in Russian], Nauka, Moscow (1981).
8. V. M. Zalkind, O. S. Pavlichenko, and V. P. Tarasenko, "Measuring the electron temperature in a plasma by a triple electric probe," *Vopr. Atom. Nauki Tekh., Ser. Fiz. Plazmy Probl. UTR*, No. 2, 69 (1975).
9. S. Tada, S. Takashima, M. Ito, et al., "Investigation of nitrogen atoms in low-pressure nitrogen plasmas using a compact electron-beam-excited plasma source," *Jpn. J. Appl. Phys., Pt. 1*, **41**, No. 7A, 4691–4695 (2002).
10. D. D. Blackwell, S. G. Walton, D. Leonhardt, et al., "Probe diagnostic development for electron beam produced plasmas," *J. Vac. Sci. Technol., Ser. A*, **19**, Part 1, No. 4, 1330–1335 (2001).
11. C. Rosenblad, H. R. Deller, A. Dommann, et al., "Silicon epitaxy by low-energy plasma enhanced chemical vapor deposition," *J. Vac. Sci. Technol., Ser. A*, **16**, No. 5, 2785–2790 (1998).
12. Q. Lin, X. Lin, Y. Yu, et al., "Measurements in silane radio frequency glow discharges using a tuned and heated Langmuir probe," *J. Appl. Phys.*, **74**, No. 8, 4899–4902 (1993).
13. R. G. Sharafutdinov, V. M. Karsten, A. A. Polisan, et al., "Method for carrying out homogeneous and heterogeneous chemical reactions using plasma," Patent No. AU2002332200, IC WO 03068383, Publ. 08.21.2003.
14. S. Tada, S. Takashima, M. Ito, et al., "Measurement and control of absolute nitrogen atom density in an electron-beam-excited plasma using vacuum ultraviolet absorption spectroscopy," *J. Appl. Phys.*, **88**, No. 4, 1756–1759 (2000).
15. R. G. Sharafutdinov, V. M. Karsten, S. Ya. Khmel, et al., "Epitaxial silicon films deposited at high rates by gas-jet electron beam plasma CVD," *Surface Coat. Technol.*, **174/175**, 1178–1181 (2003).